High temperature oxidation behavior of nanostructured Ni–Al coatings on superalloy

Atikur Rahman [a], R. Jayaganthan [a,*], Satya Prakash [a],
Vipin Chawla [a,b], Ramesh Chandra [b]

[a] Department of Metallurgical and Materials Engineering, Indian Institute of Technology Roorkee, Roorkee 247667, India
[b] Institute Instrumentation Centre & Centre of Nanotechnology, Indian Institute of Technology Roorkee, Roorkee 247667, India

ARTICLE INFO

ABSTRACT

The high temperature oxidation behavior of magnetron sputtered Ni–Al coatings on the superalloy substrate has been studied in the present work. The microstructural and morphological features of Ni–Al coatings were characterized by FE-SEM, AFM and XRD. Thermo gravimetric technique was used to investigate the oxidation behavior of the coatings, in air at 900 °C. The growth kinetics of oxide layers was predicted from the weight changes of the coating samples measured during oxidation. It was found that the corrosion rate of nanostructured Ni–Al coated superalloy was lower than that of the uncoated superalloy due to the formation of continuous, dense, adherent and protective oxide scale over the surface of the coatings. The morphological features and phases of the corroded coatings were used to elucidate the mechanism of high temperature oxidation. A continuous thin layer of protective oxide films such as NiO and Al_2O_3 has formed over the Ni–Al coatings exposed to air at high temperature, 900 °C.

© 2008 Elsevier B.V. All rights reserved.

1. Introduction

Superalloys find extensive use in gas turbines, especially for fabricating hot section components to provide superior strength and creep resistance in high temperature environment. During operation, blades and vanes of gas turbines are subjected to severe thermal cycling and mechanical loads. In addition, they are also attacked chemically by both high temperature oxidation and hot corrosion. It is impossible to impart both high temperature strength and high temperature oxidation resistance to the superalloys simultaneously along with ease of manufacturing. It is possible only with the composite materials to meet such requirements, where the base material provides the necessary mechanical strength and the coating provides the protection against wear, erosion–corrosion, and oxidation [1–3]. Therefore, protective superalloy coatings are currently used on superalloys in energy conversion and gas turbines to protect their surfaces from oxidation and hot corrosion. However, to realize the enhanced efficiency, which is unattainable with the conventional coatings, of gas turbine engines, nanostructured coatings with superior performance in terms of high temperature oxidation resistance and thermo-mechanical fatigue life are required. It is well known in the literature that the nanostructured coatings provide a better corrosion resistance at high temperature due to the formation of continuous protective layer assisted by the enhanced diffusivity of atoms in the coating [4–9].

Nanostructured coatings based on NiAl could be used for providing better high temperature oxidation protection to the superalloys as compared to the microcrystalline coatings. The B2 intermetallic compound (β-NiAl), possesses many attractive properties such as low density (approximately 5.9 gm/cm³) as compared to MCrAlY base coating, high melting point (approximately 1995 K), good oxidation resistance and metal like electrical and thermal conductivity [10–12]. Hence, thin film materials based on β-NiAl have been used for a wide variety of engineering applications such as under layers in magnetic recording media and high temperature protective coatings [13,14]. For instance, NiAl is the basis of a family of oxidation and corrosion-resistant coatings that have been used on Ni-based and Co-based superalloys. However, the high temperature oxidation behavior of nanostructured Ni–Al coatings on Ni-based super alloy substrate is scarce in the literature. Therefore, the present work has been focused to study the oxidation behavior of magnetron sputtered Ni–Al coating on the Superni-718 superalloy. The Ni–Al coatings were deposited by DC/RF magnetron sputtering. The micro structural features of the coatings were characterized by FE-SEM/EDS and AFM. XRD was used to identify the different phases in the Ni–Al coating. Thermo gravimetric technique was used to study the kinetics of high temperature oxidation behavior of the Ni–Al coating as well as bare superalloy substrate

Table 1
Chemical composition of the superalloy (Superni-718)

Midhani grade alloys	Chemical composition (wt%)											
	Fe	Ni	Cr	Ti	Al	Mo	Nb	Mn	Si	Co	S	C
Superni-718	19.8	Bal	17.6	0.96	0.53	3.23	4.91	0.02	0.03	0.01	.007	0.02

in air at 900 °C. The morphology of corroded products of coating and bare superalloy substrate was characterized by FE-SEM. The improved corrosion resistance of nanostructured Ni–Al coating exposed to high temperature environment is discussed in the present work.

2. Experimental

2.1. Deposition of Ni–Al coatings by sputtering technique

Ni-based superalloy namely Superni-718 has been chosen to deposit Ni–Al coating in the present work. The superalloy was procured from Mishra Dhatu Nigam Limited, Hyderabad, India in annealed and cold rolled sheet form and its chemical composition is shown in Table 1. Each specimen measuring approximately: 18 mm (length) × 15 mm (width) × 3 mm (thickness) were cut from the rolled sheet and polished by using 220, 320, 1/0, 2/0, 3/0, 4/0 grid SiC emery papers. Commercially available Ni Targets (99.99% pure) with dimension 2 in. diameter and 1.0 mm thickness and similarly, commercially available Al Target (99.99% pure) with 2 in. diameter and 5.0 mm thickness were fixed at an angle of 45° to each other and with the use of rotator, the substrate heater was rotated between Ni and Al targets continuously to perform a co-sputtering. The target to substrate distance was fixed at 40 mm to perform deposition. Before starting the deposition, the targets were pre-sputtered for 15 min with a shutter located in between the targets and the substrate. The shutter is also used to control the deposition time. Before deposition of Ni–Al coating, all samples were cleaned in acetone, ethanol and deionized water. The process parameters used in DC/RF magnetron sputtering are shown in Table 2.

2.2. Characterization of Ni–Al coatings

XRD (Bruker AXS) measurements with Cu Kα radiation were performed to characterize the bare and coated superalloy samples as well as the corroded products of the bare alloy and coatings to identify the different phases. The scan rate used was 2°/min and the scan range was from 10° to 110°. The grain size of the coatings was estimated from the Scherrer formula, as given in Eq. (1). In this expression, the grain size D is along the surface normal direction, which is also the direction of the XRD diffraction vector.

$$D = \frac{0.9\lambda}{B \cos \theta} \tag{1}$$

where B is the corrected full width at half maximum (FWHM) of a Bragg peak, λ is the X-ray wavelength, and θ is the Bragg angle. B is obtained from Eq. (2)

$$B^2 = B_r^2 - B_{strain}^2 - C^2 \tag{2}$$

where B_r is the FWHM of a measured Bragg peak, $B_{strain} = \varepsilon \tan\theta$ is the peak broadening from the residual strain ε measured by XRD using the $\cos^2 \alpha \sin^2 \psi$ method, and C is the instrumental line broadening [15,16].

The surface topographical characterizations of the Ni–Al coatings were made by using FE-SEM (FEI, Quanta 200F) at an acceleration voltage of 20 KV and AFM (NT-MDT, Ntegra) analysis operated in a semicontact (tapping) mode.

2.3. High temperature oxidation studies

The bare and Ni–Al coated superalloy samples were kept in the alumina boats and then inserted inside SiC tube furnace. The bare substrate specimens were mirror-

polished before oxidation. Cyclic oxidation studies were performed in air with each cycle consisting of 1 h of heating at 900 °C followed by 30 min of cooling at room temperature for up to 50 cycles. The purpose of imposed cyclic loading was to create the aggressive conditions, similar to the actual conditions, for corrosion testing. The weight changes were monitored, using an electronic balance Model CB-120 (contech, Mumbai, India) with a sensitivity of 1 mg. During each cycle, the data taken for bare and coated samples were used to calculate the corrosion rate. As spalled scale if any was also included in weight change measurements. The kinetics of oxidation was determined from the weight change measurements. After oxidation studies, the corroded samples were analyzed by using XRD and SEM/EDS techniques.

3. Results and discussions

3.1. Visual observation

The bare alloy upon exposure to high temperature oxidation showed a brownish grey color after the completion of 5th cycle and subsequently it transformed into dark grey color after the completion of 20th cycle. The coated sample showed a blue color and brown color after 5th cycle and 20th cycle, respectively. The appearance of different color over the samples indicates the formation of different oxide scale on the materials.

3.2. XRD and AFM analysis of the coatings

The XRD pattern of as deposited Ni–Al coatings on Superni-718 at different substrate temperatures are shown in Fig. 1(a). The formation of phases such as AlNi₃, NiAl and Al₄Ni₃ are observed and
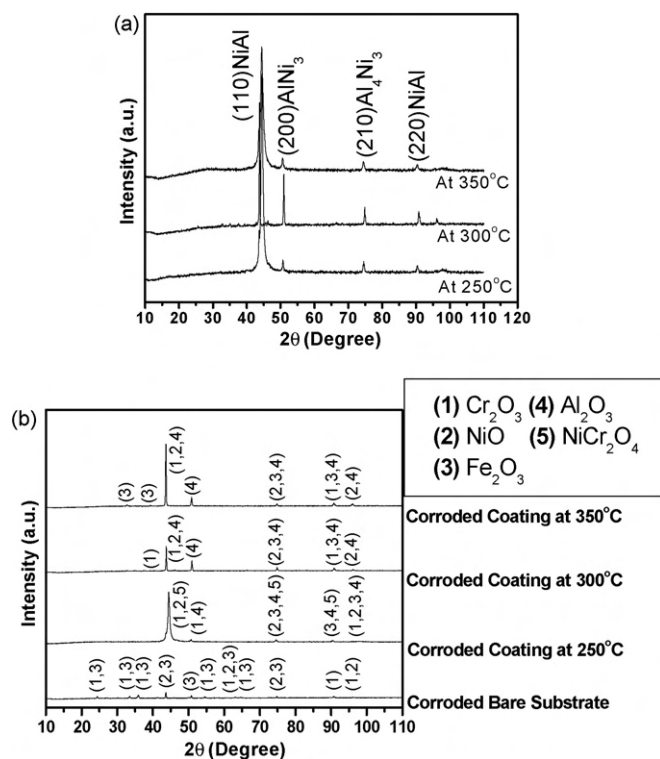
Fig. 1. XRD pattern of (a) as deposited Ni–Al coatings and (b) corroded Ni–Al coatings on bare Superni-718 and uncoated sample at different substrate temperatures.

Table 2
Sputtering parameters for Ni–Al coatings

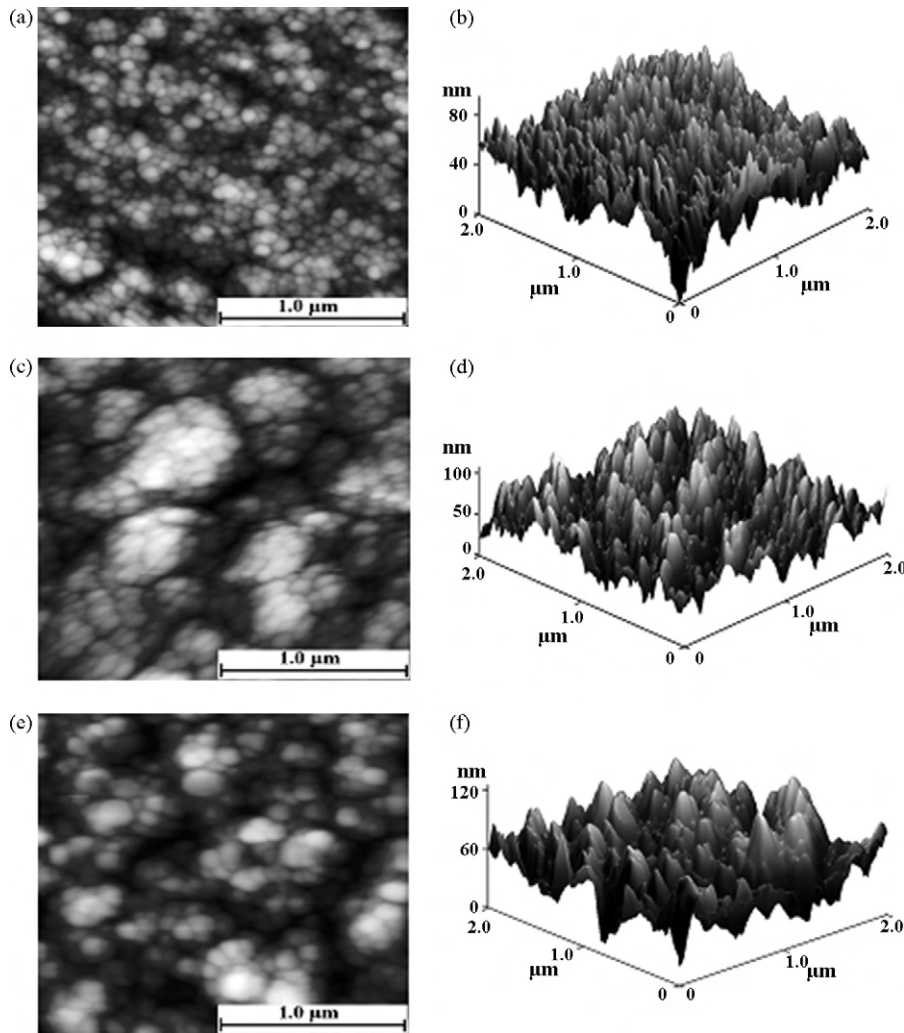| Sputtering conditions	Parameters
Target	Ni (99.99% pure, 2 in. diameter and 1 mm thickness)
	Al (99.99% pure and 2 in. diameter and 5 mm thickness)
Base pressure	3×10^{-6} Torr
Sputtering gas pressure	10 mTorr (Argon)
Sputtering power	75 W/85 W (Ni/Al target)
Substrate	Superni-718
Substrate temperature	250 °C, 300 °C and 350 °C
Deposition time	1 h

Fig. 2. AFM 2D and 3D images of Ni–Al coatings on bare Superni-718 substrate at different substrate temperatures (a–b) at 250 °C, (c–d) at 300 °C and (e–f) at 350 °C.

(1 1 0) peak of Ni–Al is dominating at different substrate temperatures. The XRD results for the corroded products of bare and Ni–Al coated samples are shown in Fig. 1(b). It is observed that the oxide scales such as Cr_2O_3, NiO, Fe_2O_3 are formed on the bare superalloy subjected to high temperature air oxidation at 900 °C and the corroded Ni–Al coating showed the presence of Cr_2O_3, NiO, Al_2O_3, Fe_2O_3, $NiCr_2O_4$. From the XRD peaks, the crystallite size of the Ni–Al coatings was found to be 17.63 nm, 39.25 nm and 10.44 nm at substrate temperatures 250 °C, 300 °C and 350 °C, respectively.

The 2D and 3D AFM images of the Ni–Al coatings at three different temperatures are shown in Fig. 2(a–f). It is observed that with increase in substrate temperature, Ni–Al coating exhibits different grain morphology. From AFM analysis, roughness of the Ni–Al coatings was found to be 8.74 nm, 16.09 nm and 15.19 nm at substrate temperatures 250 °C, 300 °C and 350 °C, respectively. The smooth surface of the coating is essential for the formation of adherent and protective oxide scales when it is exposed to high temperature environments.

3.3. Micro structural characterization of Ni–Al coating

FE-SEM images at different points on the surface of Ni–Al coating were taken and are shown in Fig. 3(a–c). It is observed that

the Ni–Al coating at substrate temperature 250 °C is porous and with increase in substrate temperature, it becomes denser. Thickness of Ni–Al coating is approximately 0.87 μm, which is calculated by using its cross-sectional FE-SEM images. The formation of the denser coatings is due to the influence of the deposition temperature and power used during sputtering.

3.4. High temperature cyclic oxidation studies in air

The weight gain per unit area versus number of cycle's plots for the bare substrate and Ni–Al coatings deposited at different substrate temperatures 250 °C, 300 °C and 350 °C on Superni-718 subjected to high temperature air oxidation studies at 900 °C is shown in Fig. 4(a). It is shown that under cyclic conditions, the bare substrate is more prone to corrosion/oxidation attack. The weight changes data as function of number of cycles are analyzed to obtain the nature of its kinetics. The parabolic rate constant is calculated from the slope of the linear regression fitted line from (weight gain/area)^2 versus number of cycles shown in Fig. 4(b). There is a visible deviation from the parabolic rate law in case of bare Superni-718 as well for the coated sample deposited at 250 °C up to 50 cycles. The weight gain data for the bare samples shows that it is prone for continuous oxidation.
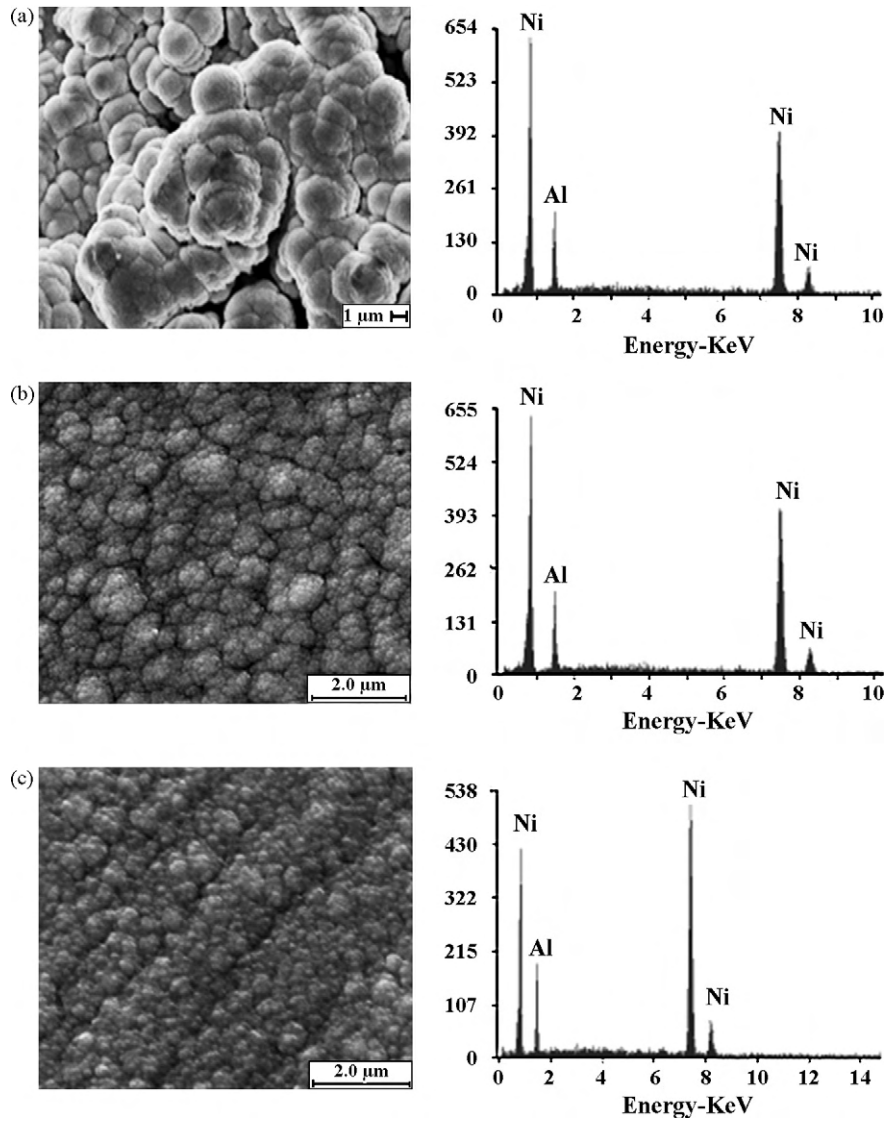
Fig. 3. FE-SEM/EDS Micrographs of Ni–Al coatings on bare Superni-718 substrate at different substrate temperatures (a) at 250 °C, (b) at 300 °C and (c) at 350 °C.
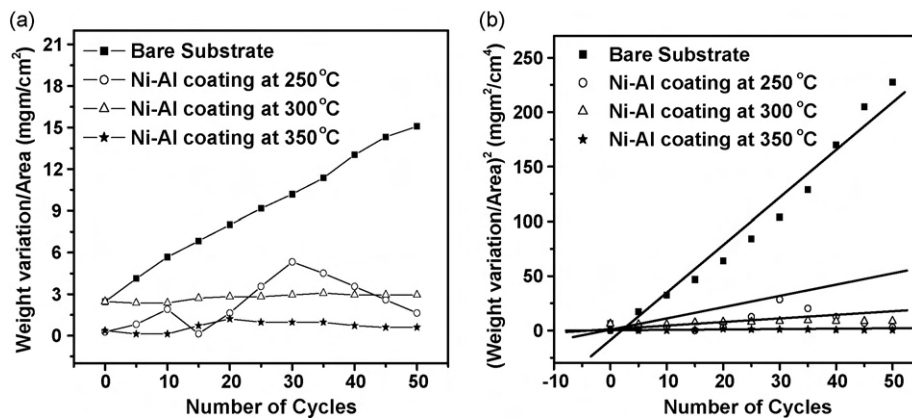

Fig. 4. (a) Weight changes/area (mg m/cm^2) versus number of cycles and (b) parabolic rate constant, K_P (weight change/area)^2, mg m^2/cm^4 versus number of cycles, for bare and coated samples oxidized in air at 900 °C.
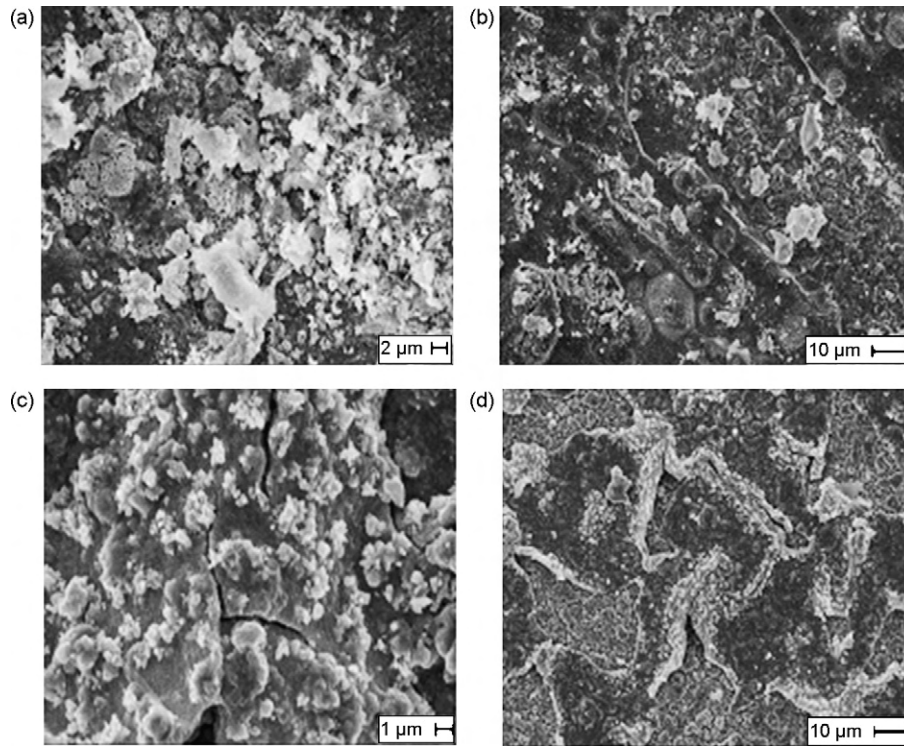
Fig. 5. (a–d) FE-SEM micrographs at the different locations of corroded bare Superni-718 substrate.

The higher weight gain of bare alloy after 30 cycles is due to spallation of initial oxide scales and the continuous exposure of fresh surface of the materials during oxidation. The evaporation of volatile impurities in the coating, during high temperature exposure, result in the formation of pores, which might also contribute to the enhanced reaction between the bare sample and oxygen. Ni–Al coating at 350 °C on Superni-718 has shown a minimum weight gain as compared to other samples of Ni–Al coating at 250 °C, 300 °C temperature and bare substrate. The calculated K_P for the Ni–Al coating at 250 °C, 300 °C, 350 °C on superalloy is found to be 0.65, 0.198 and 0.0222, respectively which is very less as compared to the K_P value of 12.51 obtained for the bare superalloy substrate. Thus, Ni–Al coating at 350 °C has provided a better protection to the Superni-718 during high temperature oxidation at 900 °C in air environment.

3.5. Surface scale analysis

FE-SEM micrographs at the selected points of interest of corroded bare substrate Superni-718 are shown in Fig. 5(a–d). The scale formed on bare Superni-718 has spalled and the cracks were formed as shown in Fig. 5(c) and (d). The large numbers of small pores on the surface of the specimen are observed from Fig. 5(a). The FE-SEM micrographs of corroded coatings are shown in Fig. 6(a–c) along with its corresponding EDS results. The oxide scale such as NiO, Al_2O_3, Cr_2O_3 and Fe_2O_3/FeO have formed on the surface of the coating as evident from EDS at the selected spot on the coating. The formation of Cr_2O_3 and Fe_2O_3 indicate the interdiffusion of the substrate elements, Fe and Cr into the coating. The scale formed on the surface of the coating is adherent and its spallation has not occurred, indicating the protective nature of the coating obeying parabolic rate of oxide growth. The nanosized grains found in the Ni–Al coating, using XRD and AFM analysis, helps in the enhanced

reactivity of Al and Ni with oxygen for the formation of continuous layer of their corresponding oxide, which is essential for providing an adequate protection to the Superni-718 in the high temperature environment. Ni–Al coating at 350 °C on Superni-718 substrate has good corrosion resistance properties as compared to coating at 250 °C and 300 °C, the reasons are as follows:

(i) As deposited Ni–Al coating is dense and continuous, which is evident from FE-SEM micrograph shown in Fig. 3(c).
(ii) An equiaxed grain morphology of the coatings is observed from the AFM analysis.
(iii) The micrographs of corroded products indicate that the oxide scale is fine, continuous, and adherent and no spallation of coating has occurred Fig. 6(a–c).
(iv) From EDS analysis, Fig. 6(a–c), it is clear that alumina content is higher in corroded Ni–Al coating at 350 °C. Thus, Al_2O_3 which is in sufficient amount on corroded surface acts as a barrier to further degradation of elements from substrate and also for oxygen and other corrosive reagents.

EDS analysis of the Ni–Al coatings Fig. 3(a–c) deposited at the substrate temperature 250 °C, 300 °C and 350 °C indicated the Al contents of 24 at%, 25 at% and 31 at%, respectively. During high temperature oxidation studies, the corner portion of the coated superalloys has corroded and spalling occurred due to the less deposition of the coating at the corner of the substrate which was fixed with a stainless clip. The EDS analysis of corroded Ni–Al coatings, deposited at 250 °C and 350 °C, showed a Al content of 20 at% and 28.3 at% in the oxide scale, respectively, as shown in Fig. 7(a) and (b). This proves that the Ni–Al coating, deposited at 350 °C, showed a lower corrosion rate as compared to that of the coatings deposited at 250 °C. It is due to the denser morphology and nanosized grains (10.44 nm) of the coatings observed at the higher deposition temperature, 350 °C. However, the weight change for
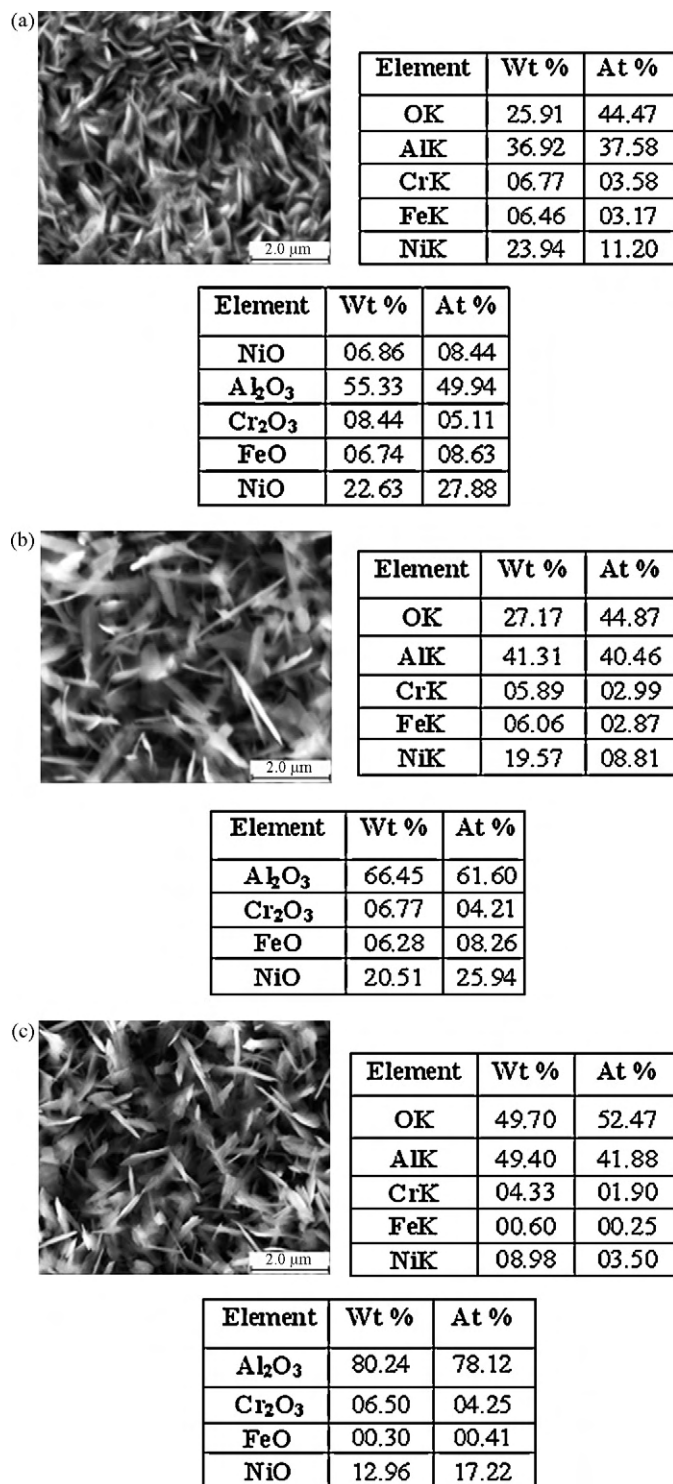
(a)

Element	Wt %	At %
OK	25.91	44.47
AlK	36.92	37.58
CrK	06.77	03.58
FeK	06.46	03.17
NiK	23.94	11.20

Element	Wt %	At %
NiO	06.86	08.44
Al_2O_3	55.33	49.94
Cr_2O_3	08.44	05.11
FeO	06.74	08.63
NiO	22.63	27.88

(b)

Element	Wt %	At %
OK	27.17	44.87
AlK	41.31	40.46
CrK	05.89	02.99
FeK	06.06	02.87
NiK	19.57	08.81

Element	Wt %	At %
Al_2O_3	66.45	61.60
Cr_2O_3	06.77	04.21
FeO	06.28	08.26
NiO	20.51	25.94

(c)

Element	Wt %	At %
OK	49.70	52.47
AlK	49.40	41.88
CrK	04.33	01.90
FeK	00.60	00.25
NiK	08.98	03.50

Element	Wt %	At %
Al_2O_3	80.24	78.12
Cr_2O_3	06.50	04.25
FeO	00.30	00.41
NiO	12.96	17.22

Fig. 6. FE-SEM Micrographs with EDS of corroded Ni–Al coatings on bare Superni-718 deposited at different substrate temperatures (a) at 250 °C, (b) at 300 °C and (c) at 350 °C.

the Ni–Al coatings deposited at 250 °C as a function of number of cycles is not constant due to the less dense morphology and higher surface roughness of the coatings, and thermal cyclic conditions. The lower corrosion rate of nanostructured NiAl coatings observed in the present work is in accordance with the results of Ren and Wang [6] who have reported the reduced the corrosion rate of the sputtered nanocrystalline NiCrAlY coatings.
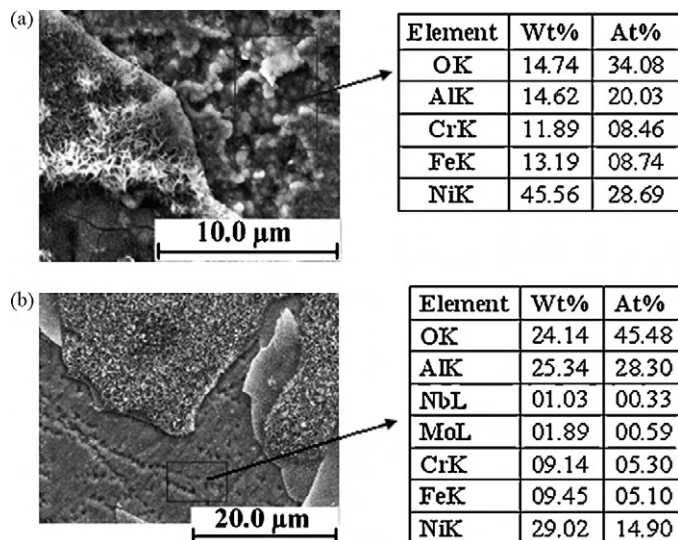
(a)

Element	Wt%	At%
OK	14.74	34.08
AlK	14.62	20.03
CrK	11.89	08.46
FeK	13.19	08.74
NiK	45.56	28.69

(b)

Element	Wt%	At%
OK	24.14	45.48
AlK	25.34	28.30
NbL	01.03	00.33
MoL	01.89	00.59
CrK	09.14	05.30
FeK	09.45	05.10
NiK	29.02	14.90

Fig. 7. EDS of corroded Ni–Al coatings on bare Superni-718 deposited at different substrate temperatures (a) at 250 °C and (b) at 350 °C.

4. Conclusions

The cyclic oxidation behavior of Ni–Al coatings, deposited on superalloy, in air environment at 900 °C has been investigated in the present work. The oxidation kinetics of Ni–Al coating was compared with that of the bare Superni-718 and found that the parabolic rate constant was very less for the former, which is due to the formation of continuous, nonporous, adherent and protective oxide scale over the surface of the coating. The continuous mass gain of bare Superni-718 is due to the spallation of initial oxide scales, renewal of fresh surface of the materials, and the pores resulting from the evaporation of volatile impurities in the alloy at high temperature. The XRD analysis of the corroded products of the Ni–Al coating indicated the formation of protective oxide scale such as Cr_2O_3, NiO, Al_2O_3, Fe_2O_3 and $NiCr_2O_4$. The morphological features of corroded coating and bare samples were characterized by FE-SEM and it was shown that the scale formed on the surface of coatings were adherent and no spallation has occurred unlike in bare samples.

References

[1] T.S. Sidhu, S. Prakash, R.D. Agrawal, Surf. Coat. Technol. 201 (2006) 273–281.
[2] M.H. Li, X.F. Sun, J.G. Li, Z.Y. Zhang, T. Jin, H.R. Guan, Z.Q. Hu, Surf. Coat. Technol. 165 (2003) 241–247.
[3] P.S. Sidky, M.G. Hocking, Corrosion 39 (1997) 511–527.
[4] S. Geng, F. Wang, S. Zhang, Surf. Coat. Technol. 167 (2003) 212–216.
[5] T.J. Nijdam, L.P.H. Jeurgens, J.H. Chen, W.G. Sloaf, Oxid. Metals 64 (2005) 355–375.
[6] X. Ren, F. Wang, Surf. Coat. Technol. 201 (2006) 30–37.
[7] G. Chen, H. lov, Corros. Sci. 42 (2000) 1185–1195.
[8] X. Peng, F. Wang, Corros. Sci. 45 (2003) 2293–2306.
[9] L. Ajdelsztajn, J.A. Picas, E. George, F.L. Kim, J. Bastian, V. Schoenung, Provenzano, Mater. Sci. Eng. A 338 (2002) 33–43.
[10] D. Zhong, J.J. Moore, E. Sutter, B. Mishra, Surf. Coat. Technol. 200 (2005) 1236–1241.
[11] D.B. Miracle, Acta Metall. Mater. 41 (1993) 649–684.
[12] R.D. Noebe, R.R. Bowman, M.V. Nathal, Int. Mater. Rev. 38 (1993) 193–232.
[13] T.J.S. Anand, H.P. Ng, A.H.W. Ngan, X.K. Meng, Thin Solid Films 441 (2003) 298–306.
[14] B. Ning, M.L. Weaver, Surf. Coat. Technol. 113 (2004) 177–178.
[15] B.E. Warren, Biscce, J. Am. Ceram. Soc. 21 (1938) 49–54.
[16] V. Chawla, R. Jayaganthan, R. Chandra, Mater. Charact., in press.